Supporting information:

"Grass-like alumina nanoelectrodes for hierarchical porous silicon supercapacitors"

Kirill Isakov[1], Olli Sorsa[2], Taina Rauhala[2], Santeri Saxelin[2], Tanja Kallio[2], Harri Lipsanen[1], Christoffer Kauppinen[1,]*

[1] Department of Electronics and Nanoengineering, Micronova, Aalto University, P.O. Box 13500, FI-00076 Aalto, Finland

[2] Department of Chemistry and Materials Science, Aalto University, P.O. Box 16100, FI-00076 Aalto, Finland

[*]Corresponding Author, e-mail: christoffer.kauppinen@gmail.com

In order to study the voltage window of the supercapacitor cells, cyclic voltammetry with increasing upper vertex voltage was performed as the first measurement for each cell. In **Figure SI1** the voltage window experiment is shown for the 50 µm PS+GLA cell and for a cell with two stainless steel spacers replacing the PS chips. Two cycles were performed with each upper vertex voltage of which the 2nd cycles are shown. There is a clear irreversible faradaic reaction dominating the current feedback of the spacer cell after 0.8 V. This is why 0.8 V was chosen as the high voltage limit. The same behavior is seen in the 50 µm PS+GLA cell which means that the voltage window of the cell is limited by the stainless steel cell components, not by the sample itself.

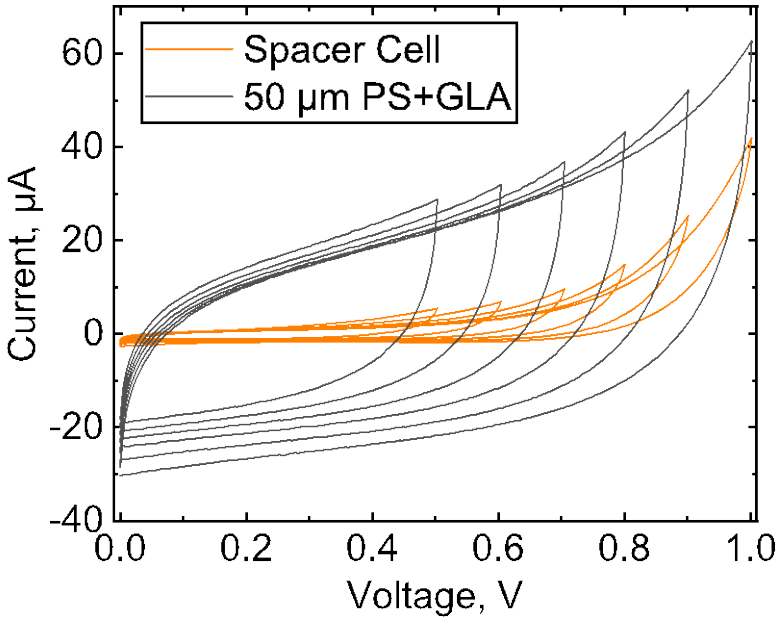

Figure SI1. Cyclic voltammograms of a cell with two spacers instead of the PS chips (spacer cell) and a cell with 50 µm PS+GLA chips. The upper vertex voltage is increased from 0.5 to 1.0 V and the scan rate is 50 mV/s.

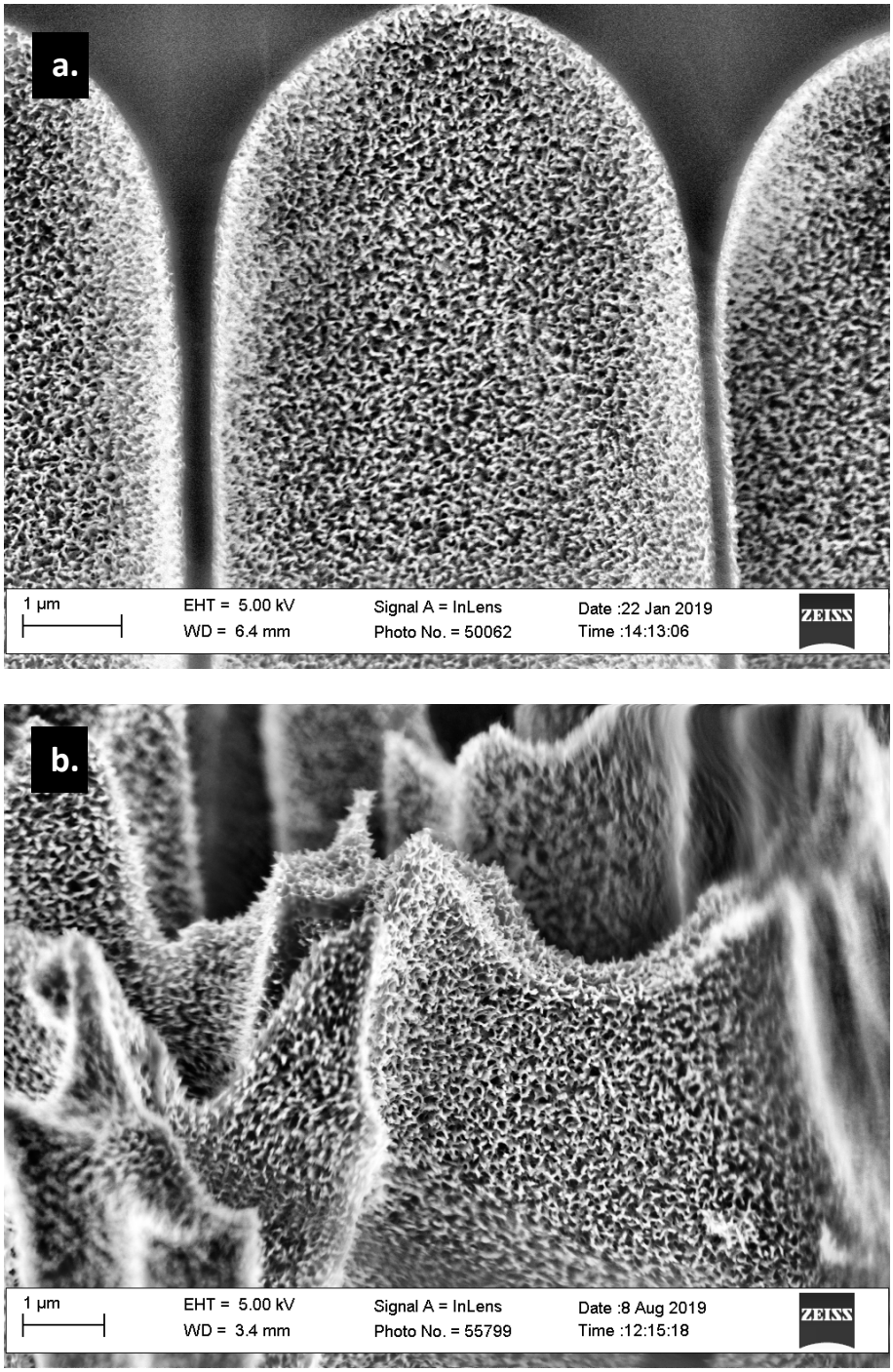

Figure SI2. Scanning electron microscope images of the GLA electrode deposited on porous silicon 200 µm deep; (a) – before the galvanostatic cycling at the bottom of porous silicon; (b) – after the galvanostatic cycling (10 000 cycles) at the top of porous silicon.

In the same spacer cell system, the conductivity of the electrolyte was tested with electrochemical impedance spectroscopy (**Figure SI3**). As a result, the area specific resistance was found to be 1.2 **Ω** cm^2 which is less than half of the ohmic resistance of the PS+GLA cells. Thus, the electrode itself hinders significantly the ohmic resistance of the system.

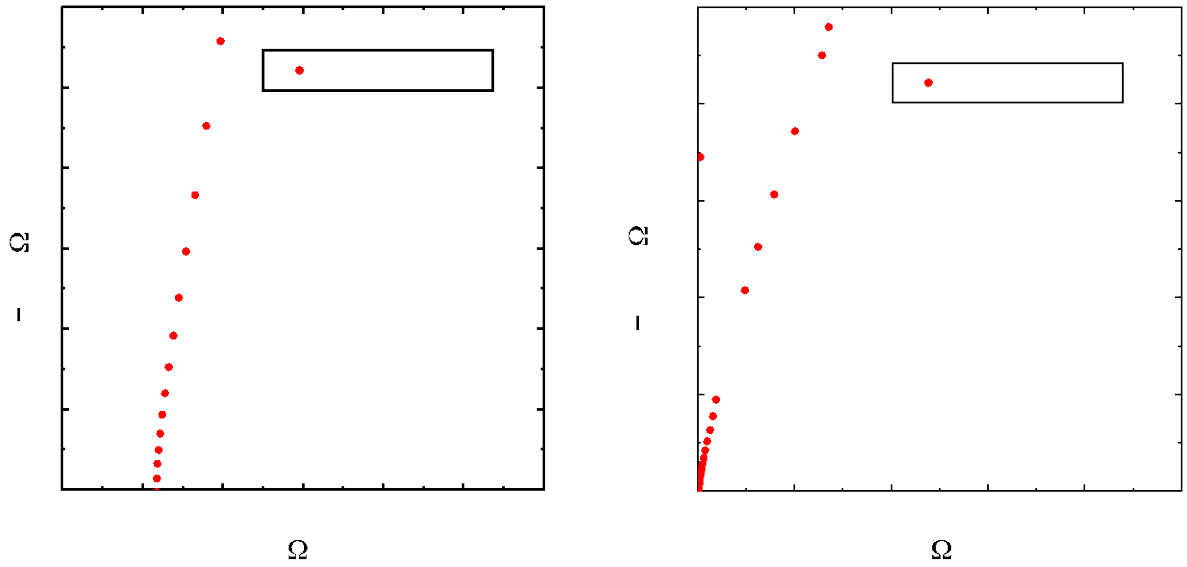

Figure SI3. Electrochemical impedance spectrum of a cell with two spacers instead of the PS chips (spacer cell).

In order to reach higher energy densities, organic electrolytes are used in supercapacitors instead of aqueous ones due to their wider potential window. The cell with 200 µm PS chips with TiN coating was tested in 1 M $TEABF_4$ in propylene carbonate but the cell did not have double layer capacitor-like behavior, as can be seen in **Figure SI4**. The cell experiences faradaic processes already at 1 V and they are enhanced after 1.8 V which is significantly lower than the expected stable potential window of the electrolyte. The cell components, including the electrodes, were dried at 110 C vacuum oven overnight prior to cell assembly in argon glove box. Consequently, there should not be substantial amounts of water left in the cell and the faradaic processes are due to the unsuitability of the electrolyte with the PS or the TiN coating.

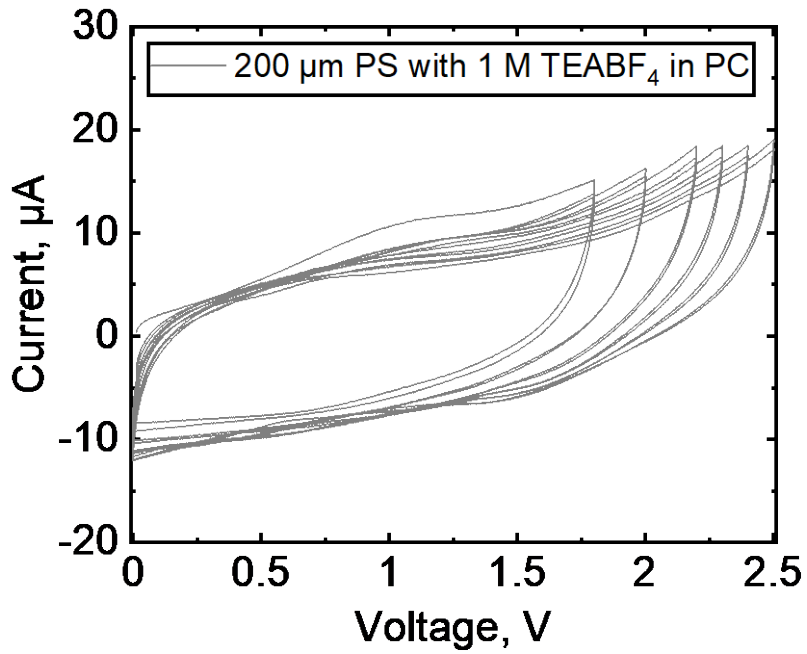

Figure SI4. Cyclic voltammogram of a cell with 200 µm PS chips in 1 M $TEABF_4$ in propylene carbonate. The upper vertex voltage is increased from 1.8 to 2.5 V and the scan rate is 50 mV/s.

For a more comlete picture of the electrochemical characteristics, the cyclic voltammograms (unnormalized and normalized with scan rate) and galvanostatic cycles (unnormalized and normalized with the applied current density) are provided below for every sample.

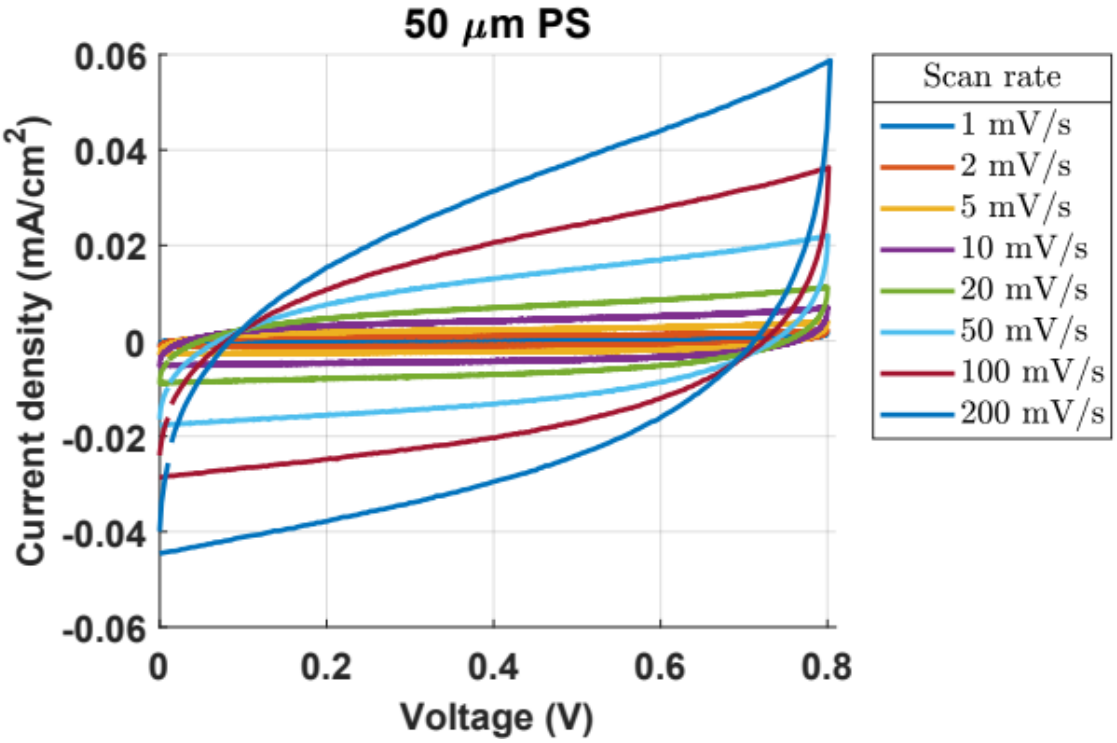

Figure S5: Cyclic voltammogram the of 50 µm PS sample.

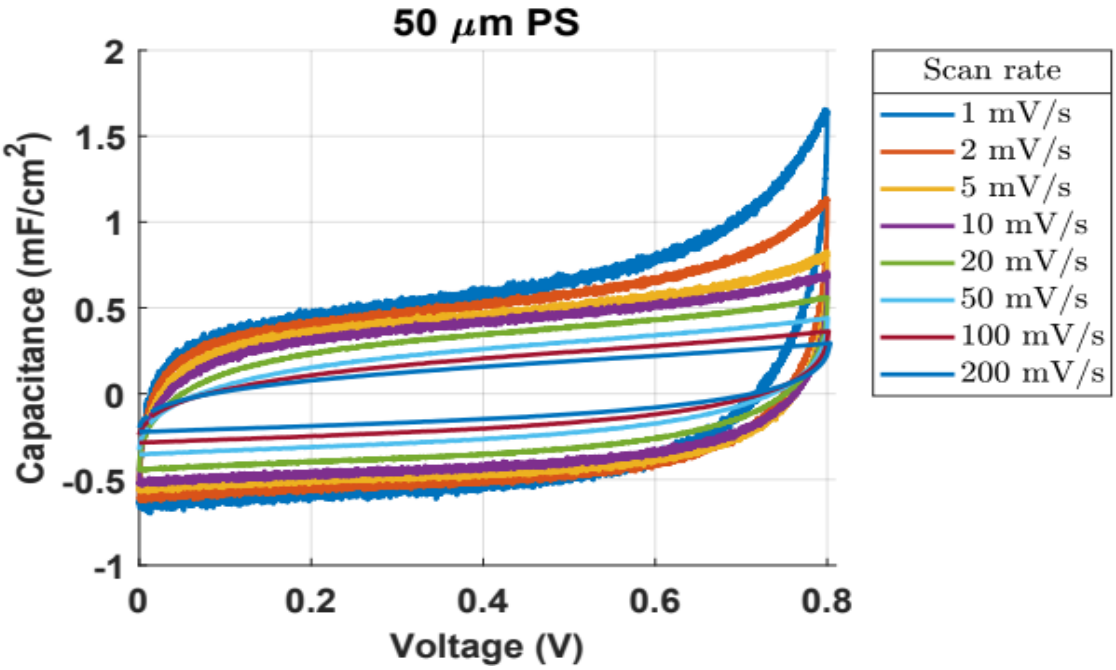

Figure S6: Cyclic voltammogram of the 50 µm PS sample normalized with the scan rate to plot the capacitance.

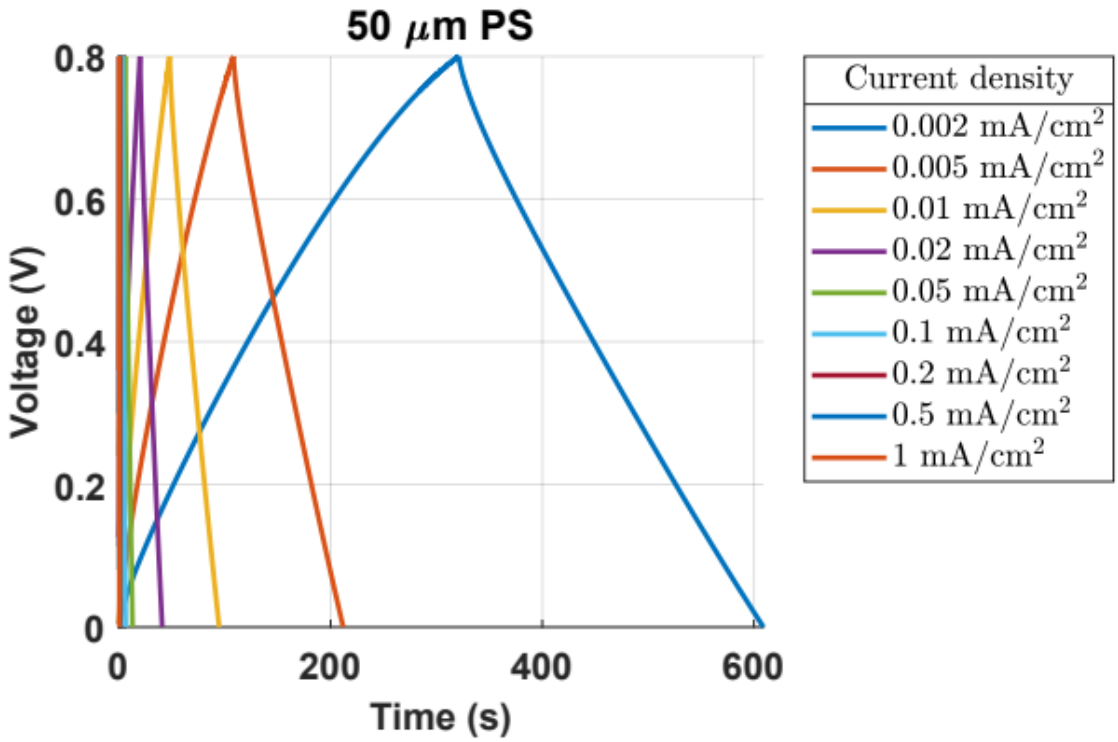

Figure S7: Galvanostatic cycles of the 50 µm PS sample.

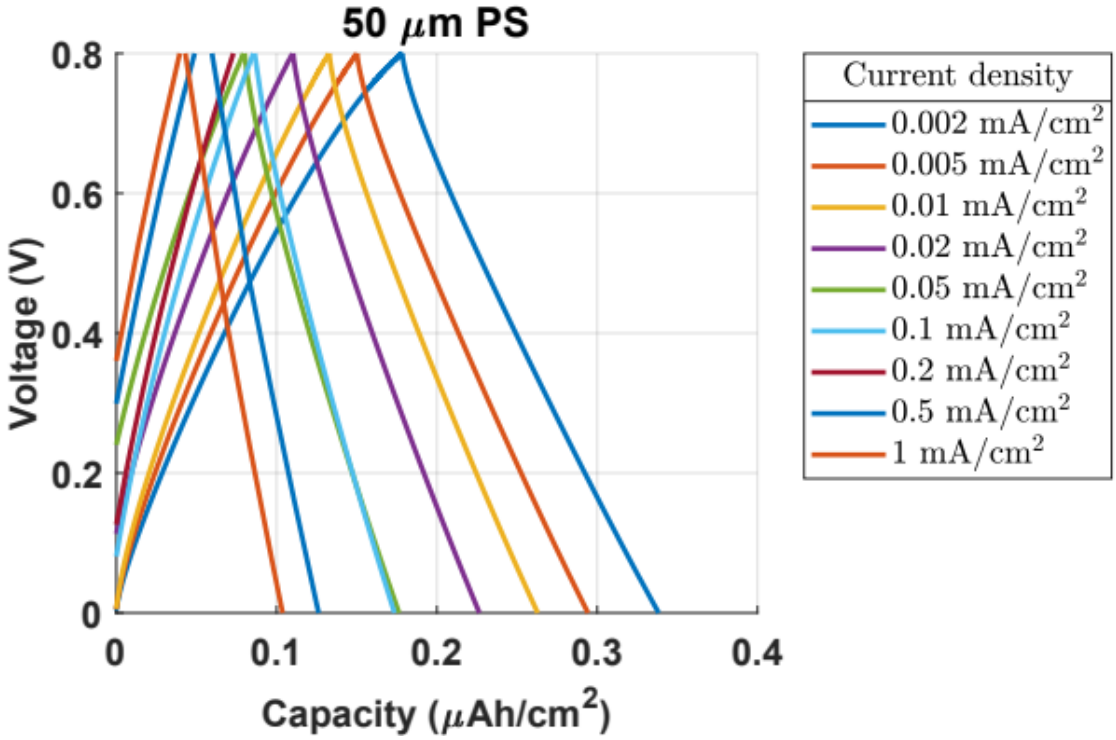

Figure S8: Galvanostatic cycles of the 50 µm PS sample normalized with the applied current density to plot the capacity.

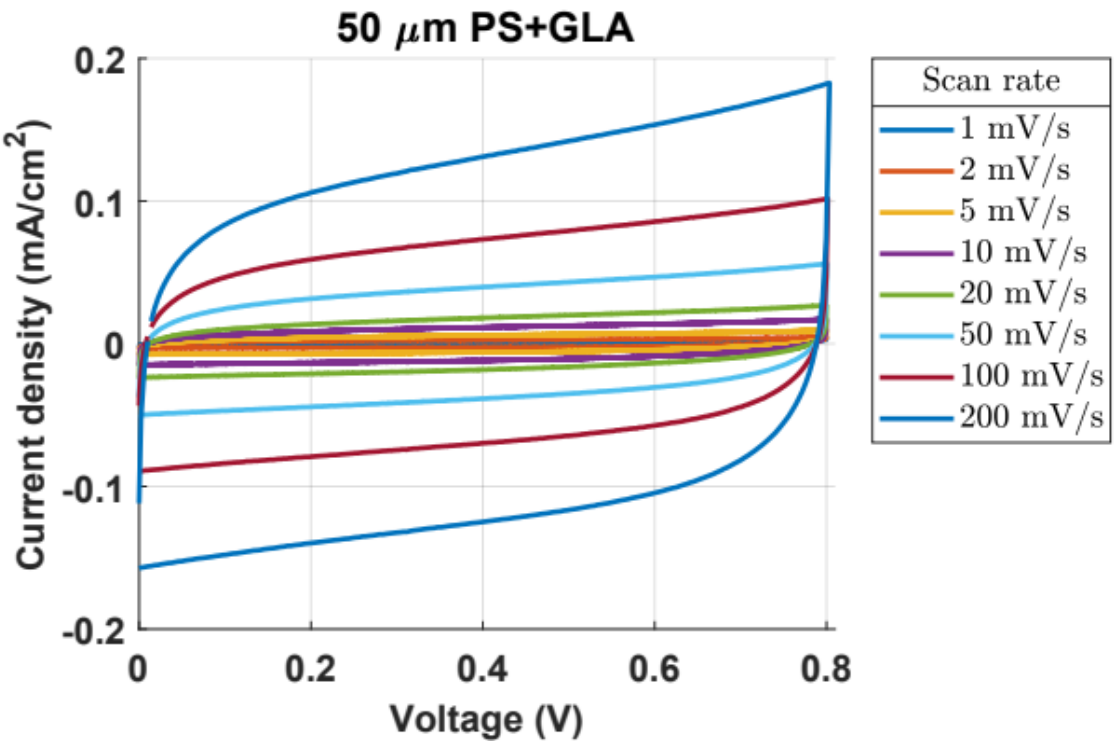

Figure S9: Cyclic voltammogram the of 50 µm PS+GLA sample.

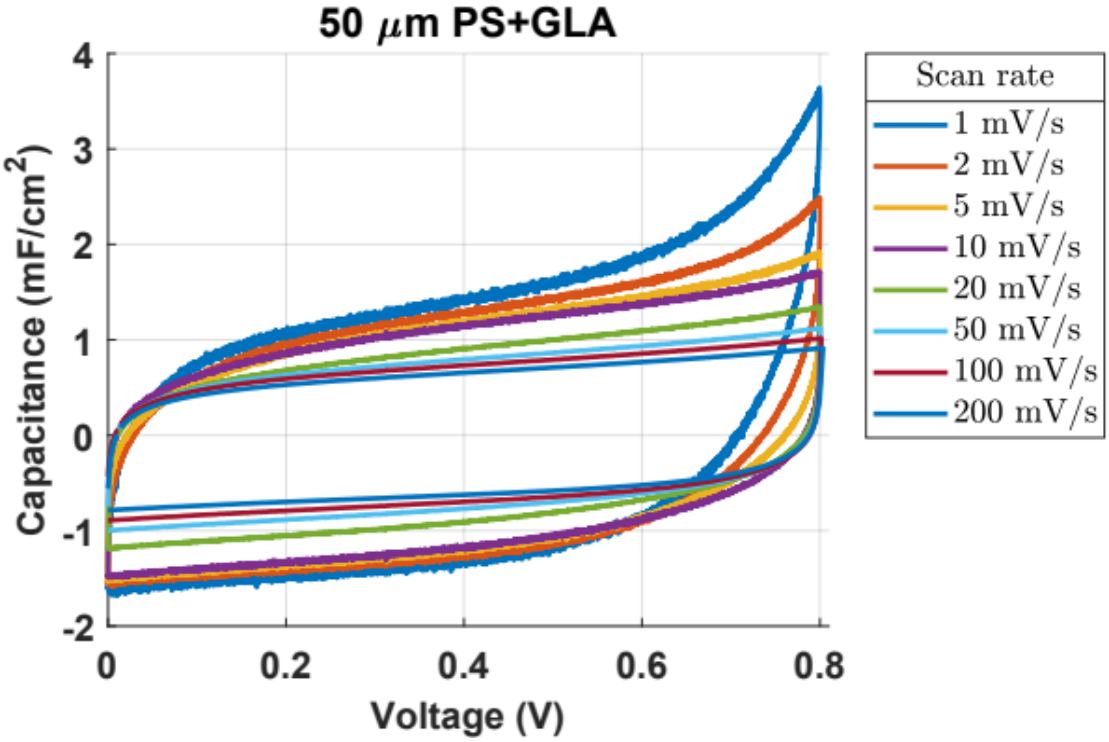

Figure S10: Cyclic voltammogram of the 50 µm PS+GLA sample normalized with the scan rate to plot the capacitance.

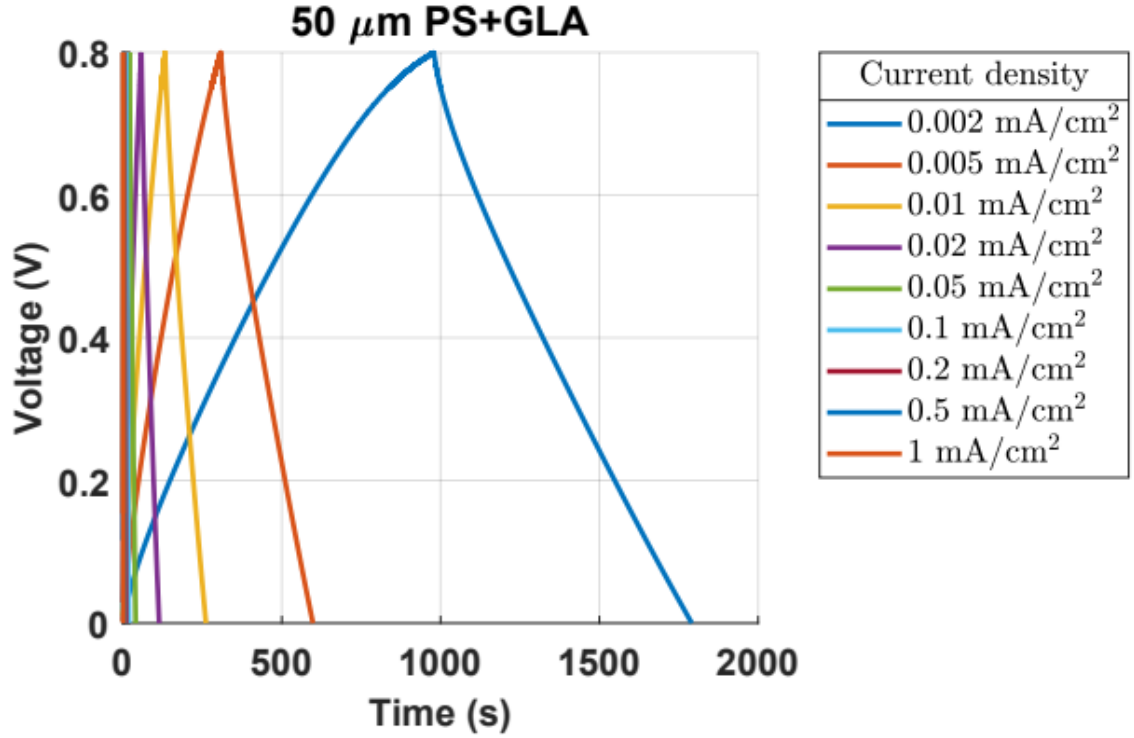

Figure S11: Galvanostatic cycles of the 50 µm PS+GLA sample.

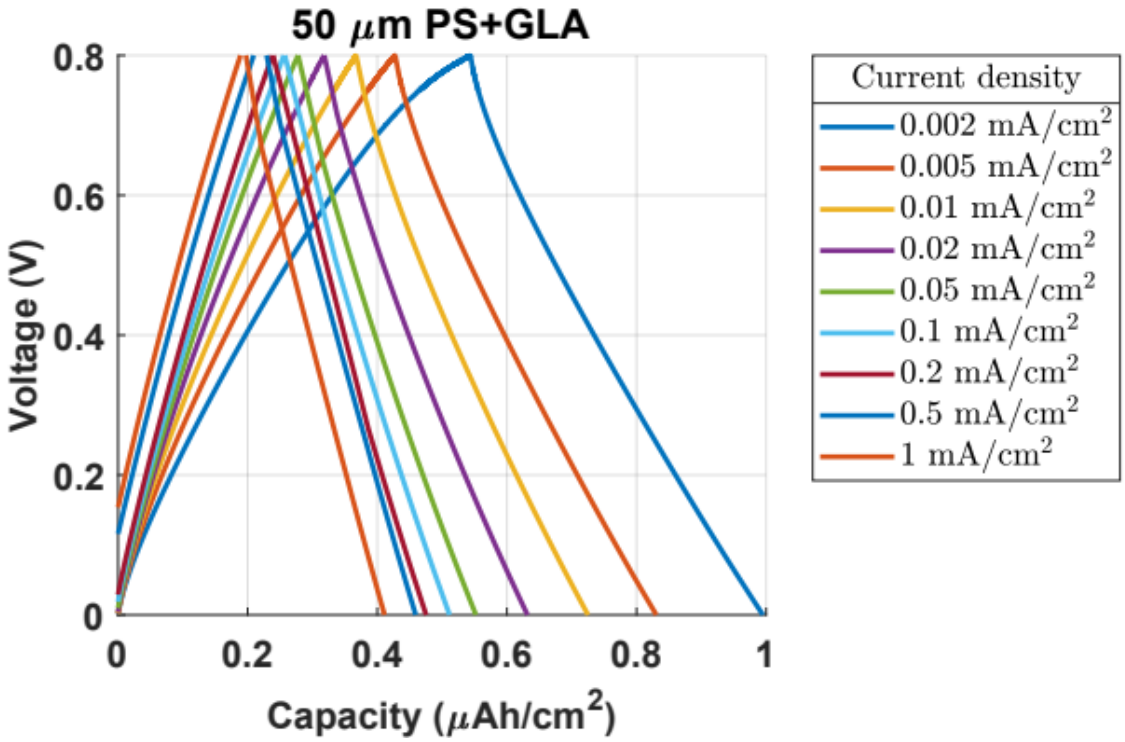

Figure S12: Galvanostatic cycles of the 50 µm PS+GLA sample normalized with the applied current density to plot the capacity.

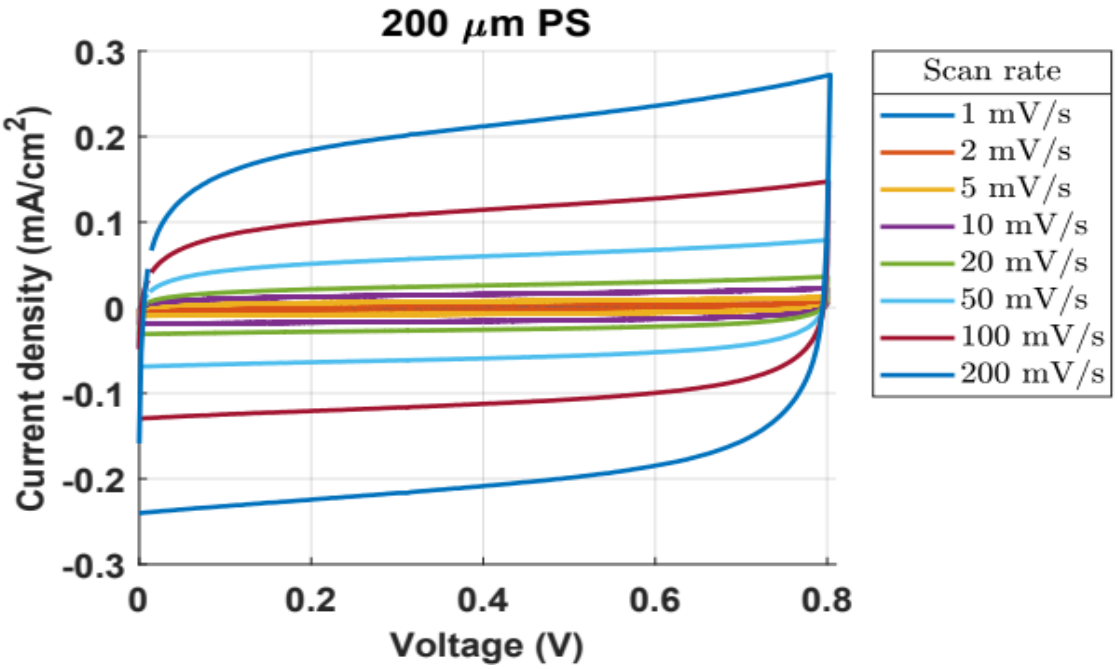

Figure S13: Cyclic voltammogram the of 200 µm PS sample.

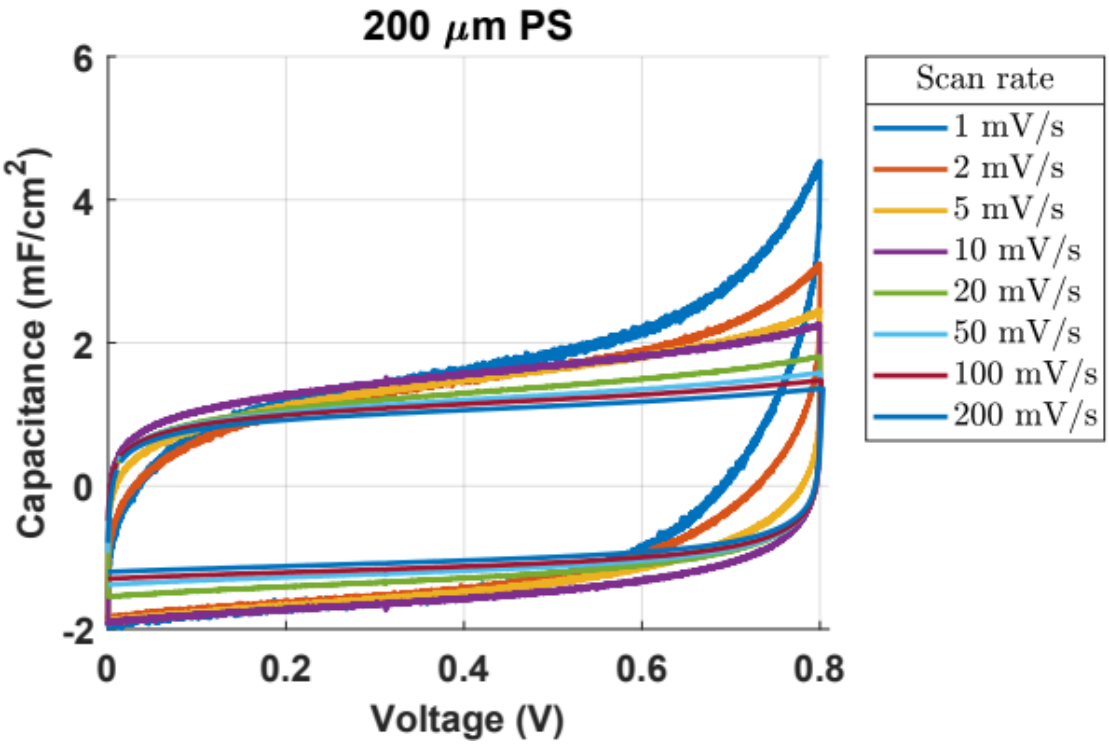

Figure S14: Cyclic voltammogram of the 200 µm PS sample normalized with the scan rate to plot the capacitance.

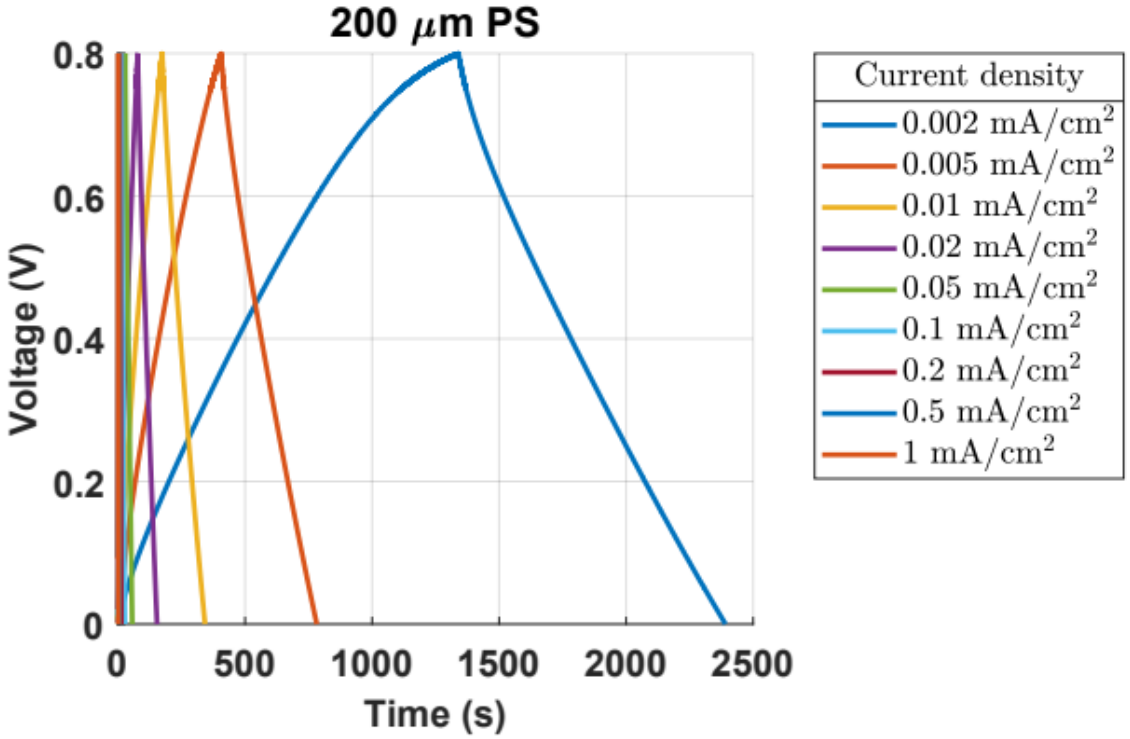

Figure S15: Galvanostatic cycles of the 200 µm PS sample.

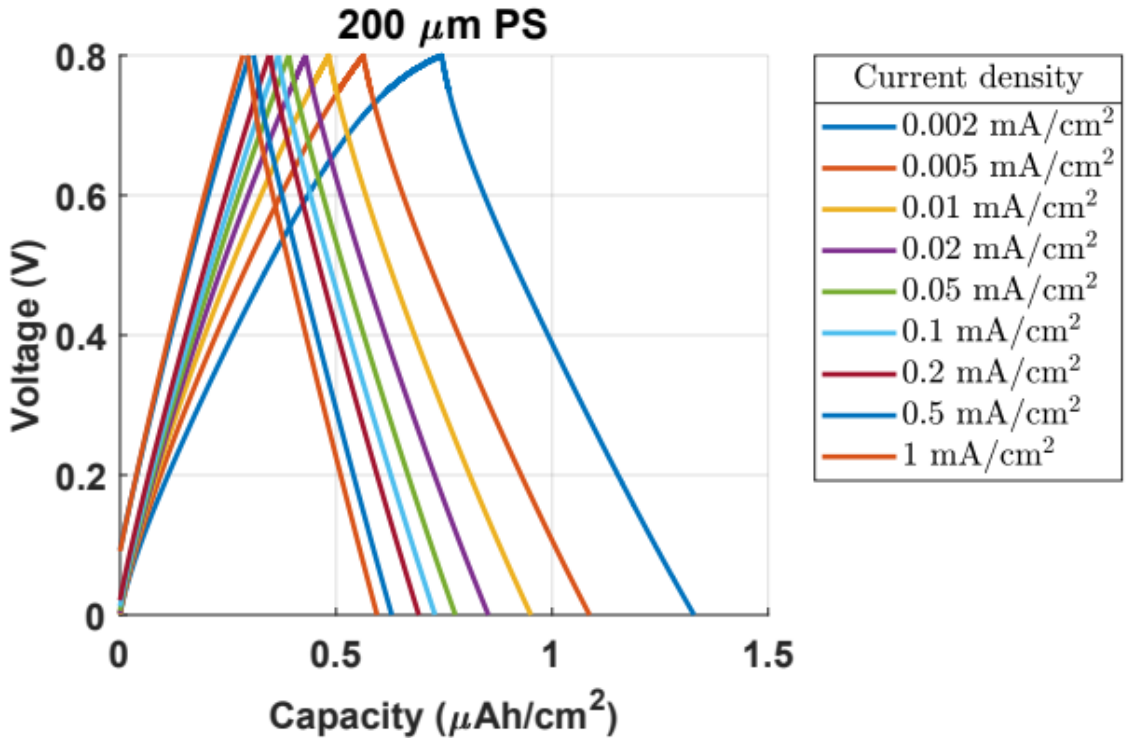

Figure S16: Galvanostatic cycles of the 200 µm PS sample normalized with the applied current density to plot the capacity.

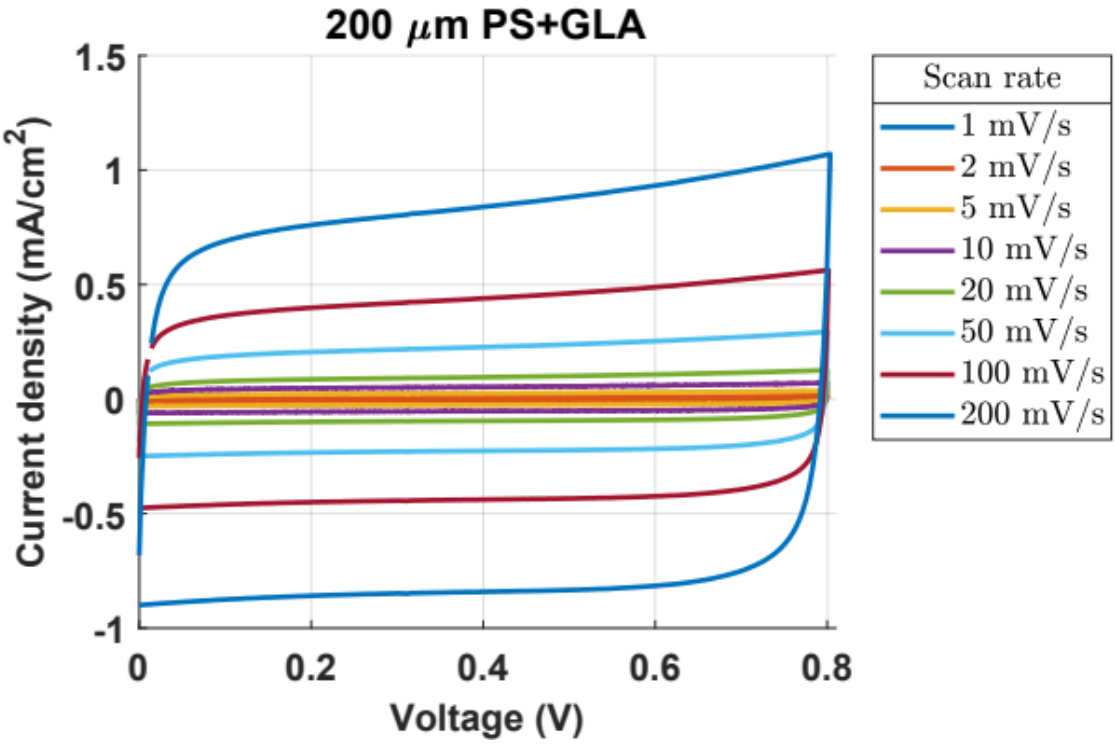

Figure S17: Cyclic voltammogram the of 200 µm PS+GLA sample.

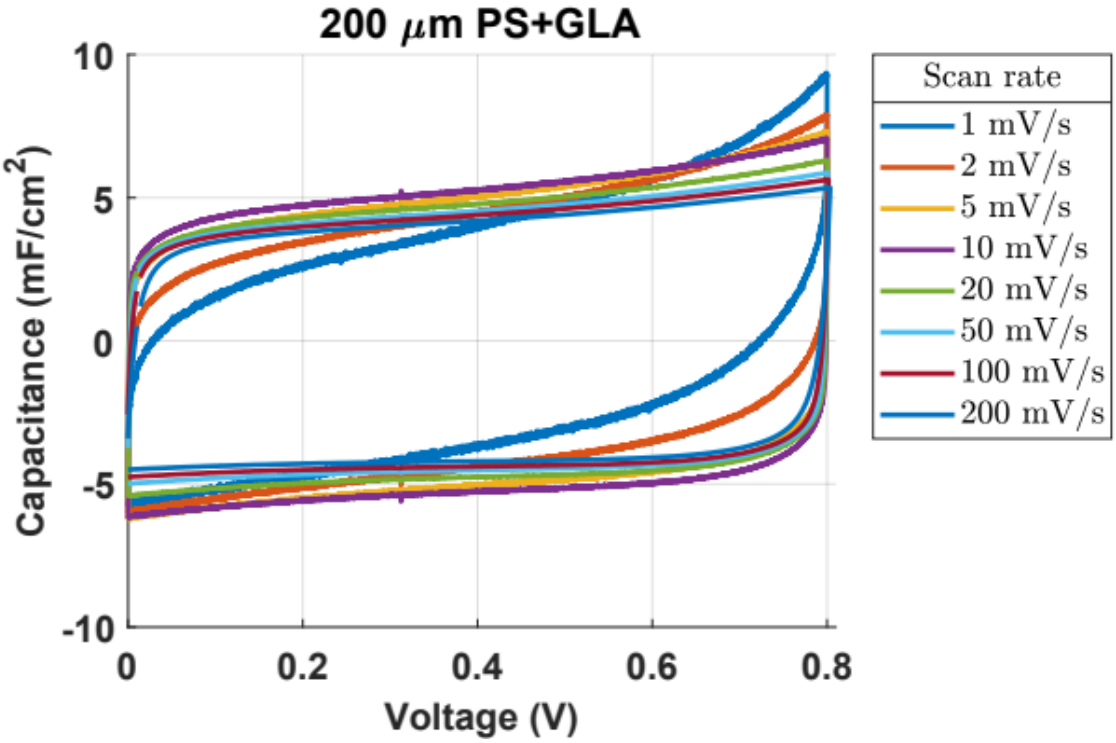

Figure S18: Cyclic voltammogram of the 200 µm PS+GLA sample normalized with the scan rate to plot the capacitance.

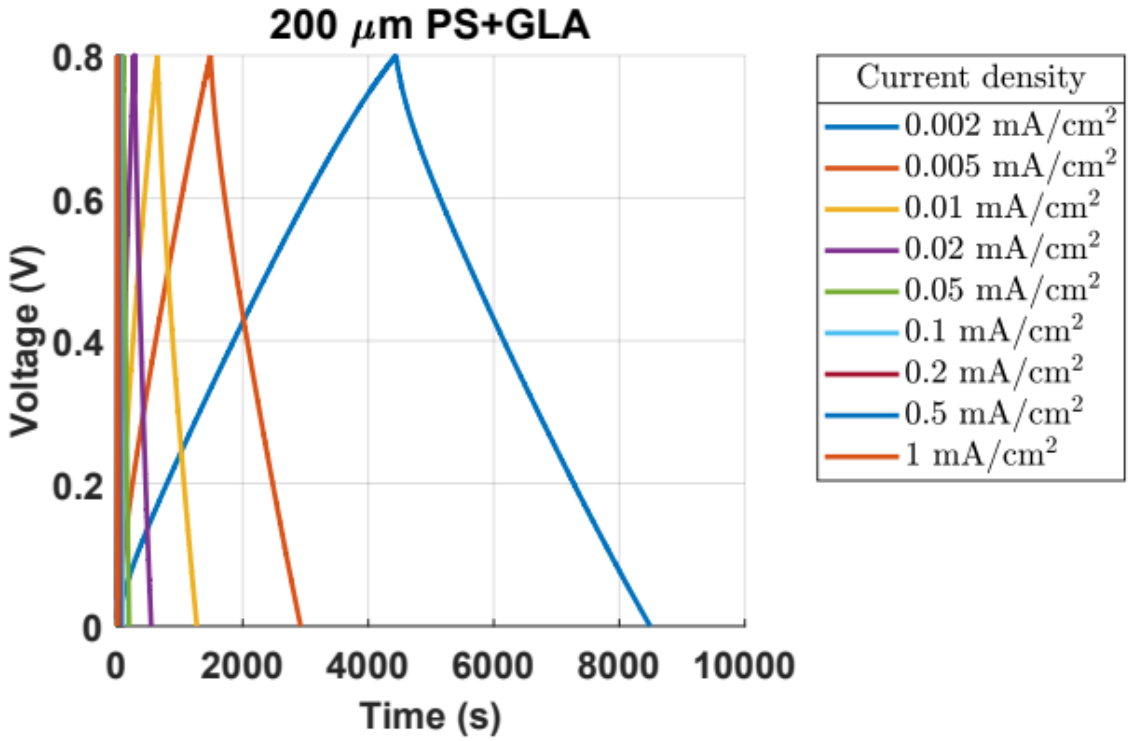

Figure S19: Galvanostatic cycles of the 200 µm PS+GLA sample.

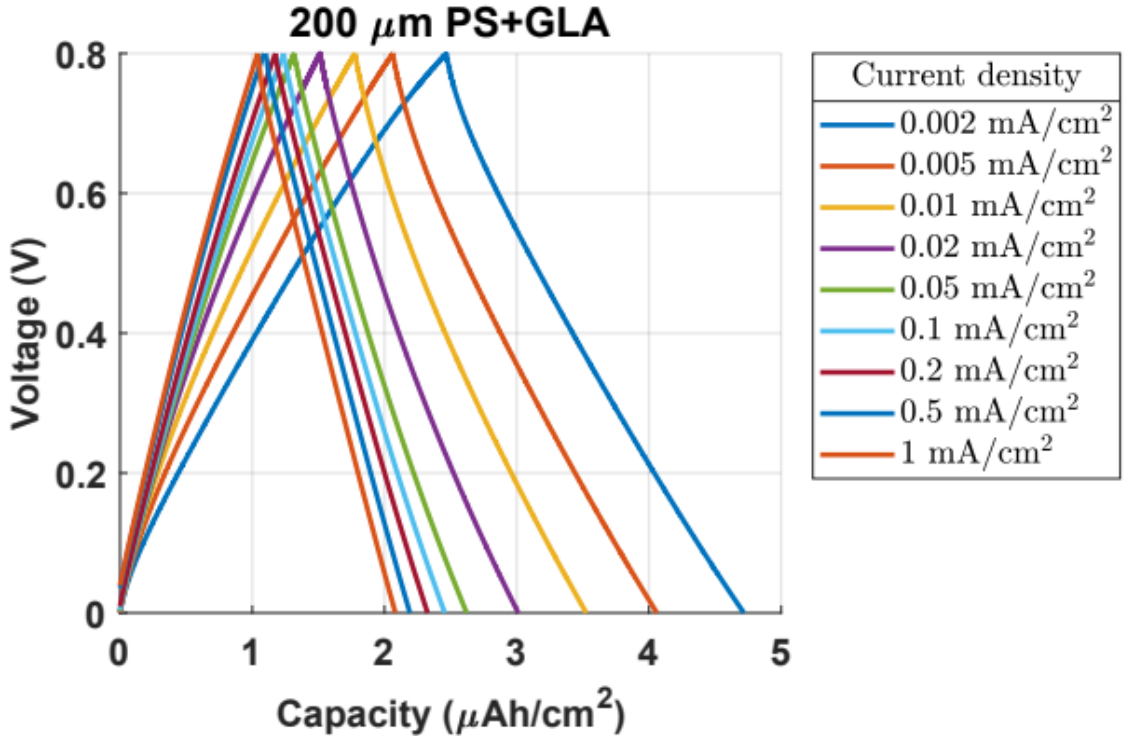

Figure S20: Galvanostatic cycles of the 200 µm PS+GLA sample normalized with the applied current density to plot the capacity.